

MONITORING OF HARMFUL ALGAL BLOOMS ALONG THE NORWEGIAN COAST USING BIO-OPTICAL METHODS

G. JOHNSEN* and E. SAKSHAUG*

A Norwegian monitoring system for harmful algal blooms, consisting of an Observer Network, the State Food Hygiene Control Agency, the Oceanographic Company of Norway, the Institute of Marine Research and the Directorate for Fisheries, is reviewed. Potentially harmful algae on the Norwegian coast are found primarily in four classes of phytoplankton, dinoflagellates, prymnesiophytes, diatoms and raphidophytes. The system consists of buoys designed for real-time, *in situ* monitoring and forecasting, and is used principally to provide an early warning to the aquaculture industry. The system allows detection of potentially toxic species, through a combination of physical, chemical, biological and bio-optical data. New datasets using bio-optical techniques on glass-fibre filters are also described, providing information on the composition and health of phytoplankton populations.

Information on existing monitoring practices for Harmful Algal Blooms (HABs) worldwide is reported in UNESCO (1996). Included in that report is an overview of the effects of HABs on marine life and aquaculture in Norway and of the system of monitoring harmful phytoplankton species. This system of monitoring provides information for mariculture and fisheries management, in addition to information on eutrophication, climate change and ecosystem damage. The system consists of an observer network of fish and mussel farmers, the State Food Hygiene Control Agency, Oceanographic Company of Norway, Trondheim – the Seawatch system, the Institute of Marine Research in Bergen, and the Norwegian Directorate for Fisheries. A weekly report on the Internet (<http://algeinfo.imr.no>) provides information on the concentration and distribution of phytoplankton, including harmful species, in five geographical zones along the Norwegian coast. The risk to marine life and the potential for toxic shellfish poisoning is also assessed (Fig. 1).

Potentially harmful phytoplankton on the Norwegian coast are found primarily in four classes of phytoplankton:

- Dinoflagellates: *Alexandrium* spp. (four species), *Amphidinium carterae*, *Dinophysis* spp. (five species), *Gymnodinium galatheanum*, *Gyrodinium* cf. *aureolum* (= *Gyrodinium mikimotoi*), *Prorocentrum* spp. (two species).
- Diatoms: *Chaetoceros* (four species), *Leptocylindrus minimus*, *Pseudo-nitzschia* spp. (three species), *Rhizosolenia* spp., *Skeletonema costatum*.
- Prymnesiophytes: *Chrysochromulina* spp. (>three species), *Phaeocystis pouchetii*, *Prymnesium* spp.

(two species).

- Raphidophytes: *Heterosigma akashiwo*, *Chattonella* sp.

The HAB monitoring programme in Norway is financed by fish farmers, in cooperation with insurance companies and the State Food Hygiene Control Agency. The value of Atlantic salmon *Salmo salar* and rainbow trout *Salmo irideus* produced by Norwegian fish farms was approximately US\$1.3×10⁹ in 1998. The cost of the HAB monitoring system, excluding the Seawatch buoy system, during that year amounted to US\$300 000, equivalent to 0.02% of the value of the salmon and trout production. The system provides the lowest monitoring cost relative to the value of production of any national programme worldwide (UNESCO 1996). The estimated economic loss attributed to HABs is approximately US\$2×10⁶ per year, i.e. 6.7 times higher than the total cost of the monitoring programme. With the additional information provided by five Seawatch buoys, situated at strategic points along the Norwegian coast, at an annual cost of US\$0.13×10⁶ each, the total cost of the monitoring is approximately 50% of the estimated economic loss attributed to HABs.

In the first part of this paper, the use of bio-optical methods in monitoring HABs is described, and an assessment of the ability of the Norwegian buoy system to provide an early warning system for HABs is assessed. In the second part, new data relating to the bio-optical properties (absorption and fluorescence) of phytoplankton and other particles is assessed to provide information on the taxonomy, physiology and health of phytoplankton populations.

* Trondheim Biological Station, Norwegian University of Science and Technology, N-7034 Trondheim, Norway. E-mail: geir.johnsen@vm.ntnu.no

General:

Low to moderate concentrations of phytoplankton are found from the northern to the southern part of Norway. The bloom of *Gyrodinium* cf. *aureolum* is in a post-bloom phase along the Skagerrak coast (S-Norway). From the Swedish border to V est Agder (S-tip of Norway): High [*Dinophysis*]: danger for toxic mussels.

Region 1-2 (Northern Norway):

There is a rise in [diatom] in the Altafjord dominated by *Chaetoceros* and *Pseudo-nitzschia*. Low [phytoplankton] at the other sampling stations. PSP-toxins found in mussels at V adsø (Finnmark county).

Region 2-3 (Mid-Norway):

The bloom of *Pseudo-nitzschia* in the Trondheimsfjord is still going on. Some minor diatom blooms in outer parts of South Trøndelag and More & Romsdal counties. PSP found in mussels in the Frøya-Hitra area.

Region 3-4 (South-West Norway):

Small to medium [diatom] in the area: 0.50×10^6 cells l^{-1} of *Skeletonema* in the Dalane and 0.35×10^6 cells l^{-1} of *Pseudo-nitzschia* in Nordflorden. The *Pseudo-nitzschia* is in a post-bloom phase in Sognefjorden (0.1×10^6 cells l^{-1}).

Region 4-5 (South-East Norway):

1.2×10^6 cells l^{-1} of *Skeletonema* are found close to the shoreline in Østfold county. *Prorocentrum minimum* is an associated species in this bloom. [*Gyrodinium* cf. *aureolum*] is in post-bloom phase in the same area. In Aust-Agder (Flødevigen station) a bloom of *Ceratium* spp. and *Chaetoceros* is registered. *Dinophysis* spp. is registered in high concentrations -toxic and potential toxic mussels.

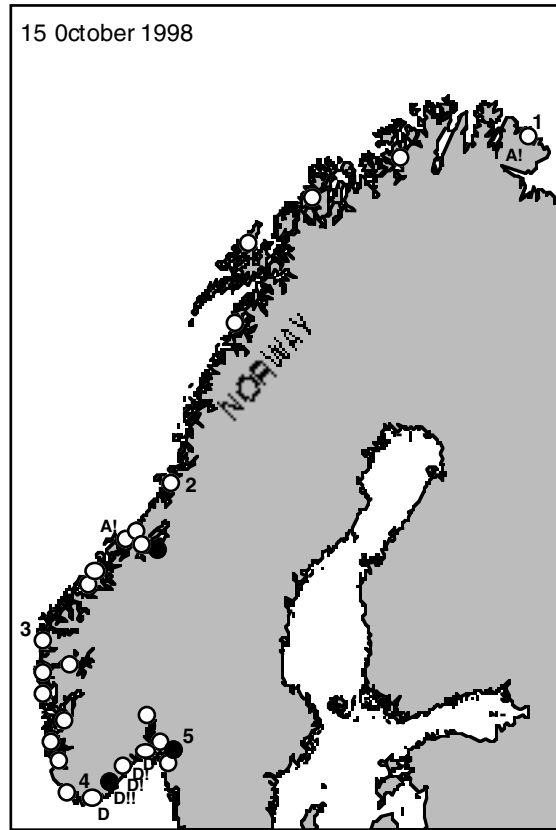


Fig. 1: HAB information on the Norwegian coast on 15 October 1998 (translated from Norwegian, <http://algeinfo.imr.no>). A database is also provided for each geographic region. Filled, half-filled and open circles denote high, medium and low phytoplankton concentrations respectively. ! and !! indicate the possible risk of toxic mussels, which may be harmful to fish. A = *Alexandrium* spp. (PSP toxins), D = *Dinophysis* spp. (DSP toxins)

MONITORING HABs USING BIO-OPTICAL METHODS

The feasibility of detecting and monitoring phytoplankton blooms, using moored equipment to measure changes in the bio-optical properties of phytoplankton, has been demonstrated by Cullen and Lewis (1995) and Johnsen *et al.* (1997b). In eukaryotic phytoplankton, the pigments are, in most cases, found within the thylakoid membranes in the chloroplasts (Fig. 2). They are the sites of light harvesting and energy utilization (photochemistry). Three major pigment groups determine the bio-optical properties of phytoplankton: the fat-soluble chlorophylls and carotenoids found in all phytoplankton classes, and

the water-soluble phyco-biliproteins found mainly in the cryptophytes, cyanobacteria and some unicellular red algae.

The identification of phytoplankton on the basis of spectral *in vivo* light absorption and fluorescence excitation spectra depends on species and group-specific differences in the pigment composition, as modified by the state of photo-acclimation (Haxo and Blinks 1950, Yentsch and Yentsch 1979, Bricaud *et al.* 1988, Mitchell 1990, Johnsen *et al.* 1994a, 1997a). The ability to detect/identify phytoplankton on the basis of spectral absorption and fluorescence depends on the wavelengths and the numbers in each measured. Five taxonomically relevant wavelengths (481, 535, 586, 628 and 649 nm) have yielded near-optimum classification success for 10 phytoplankton classes with several pigment sub-

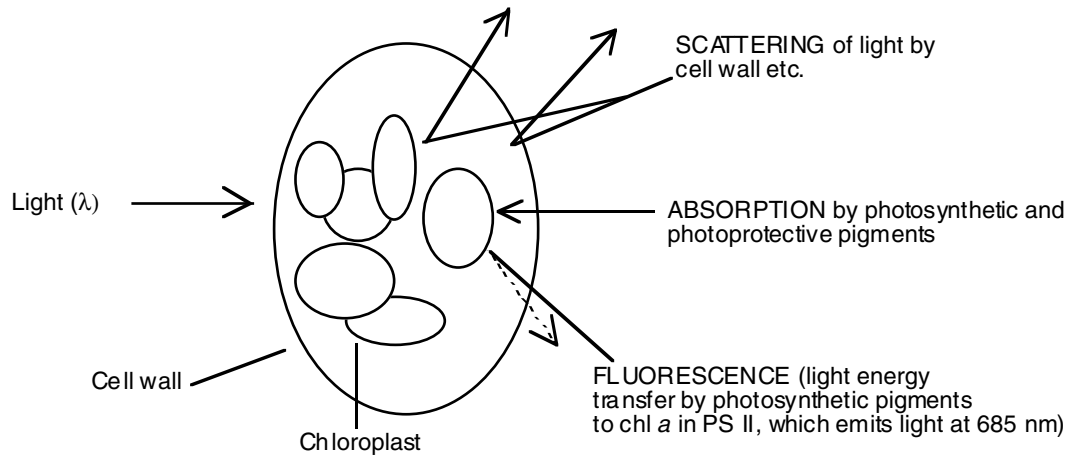


Fig. 2: Diagrammatic representation of a phytoplankton cell, showing bio-optical properties, which are determined by pigment composition, cell size, shape and morphology. Likewise, chloroplast size, shape, number, morphology and distribution, the degree of stacking and the optical properties of the thylakoid membranes contribute to differences in cellular light scattering, absorption and fluorescence

groups (Johnsen *et al.* 1994a, Table I). The Chl c_3 -group, which also contains acyloxy-fucoanthins, is optically different from the other pigment groups and indicates the presence of potentially toxic-bloom-forming prymnesiophytes and certain toxic dinoflagellates (*Gyrodinium mikimoti* and *Gymnodinium cf. galatheanum* (Fig. 3, Table I).

Discriminant analysis has been used to assess the use of this approach in the field (Table I). Water samples from several phytoplankton blooms were analysed using the same approach as that used in the laboratory

(Johnsen *et al.* 1998). The field results clearly showed the same pigment group patterns as observed in the laboratory (Fig. 3).

BUOY SENSORS AND THE OBSERVER NETWORK

The Seawatch system consists of several buoys designed for real-time, *in situ* monitoring and forecasting

Table I: Relationship between *in vivo* absorption maxima and predominant pigments at various wavelengths (Johnsen *et al.* 1994a). The wavelengths are selected by discriminant analysis, based on absorption spectra from 217 *in vivo* absorption spectra from 31 species constituting the 10 most important phytoplankton classes

Phytoplankton classes	<i>In vivo</i> absorption maxima (nm)			
	481	535	586	649
Diatoms	DD, F	F	Chl c_{1+2}	–
Dinoflagellates	DD, P/(F+19'F)	P/(F+19'F)	Chl $c_{2(3)}$	–
Prymnesiophytes	DD, F, 19'F	F, 19'F	Chl c_{2+3}	–
Prasinophytes	PR/L, V,Z, Chl b	PR	Chl $a+b$, Mg-D	Chl b
Euglenophytes	DD, N, Chl b	–	Chl $a+b$	Chl b
Chlorophytes	V, Z, L, Chl b	–	Chl $a+b$	Chl b
Chrysophytes	DD, F	F	Chl c_2	–
Raphidophytes	F, V, Z	F	Chl c_{1+2}	–
Cryptophytes	AX	PE	Chl c_2	–
Cyanobacteria	PUB, Z, β	PEB	–	–

Mg-D = Magnesium 3,8 divinyl phaeoporphyrin a_5 monomethylester, DD = Diadinoxanthin, F = Fucoxanthin, P = Peridinin, 19'F = 19'-acyloxyfucoxanthins, PR = Prasinoxanthin, V = Violaxanthin, Z = Zeaxanthin, N = Neoxanthin, L = Lutein, AX = Alloxanthin, β = β -carotene, PE = Cr-phycoerythrin 545, PUB = Phycourobilin, PEB = Phycoerythrobilin

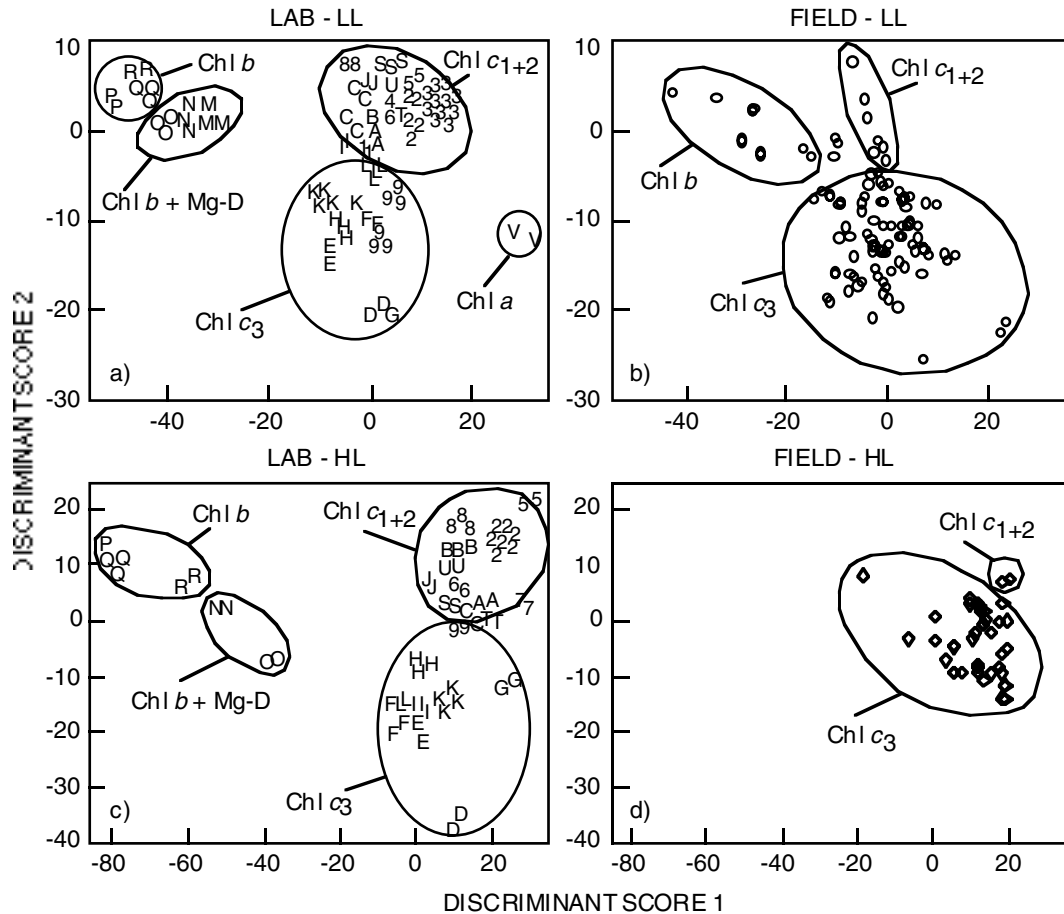


Fig. 3: Discriminant scores evaluated on logarithmically transformed and scaled absorption spectra, $a_{\log}(\lambda)$, at 481, 535, 649 nm on phytoplankton cultures that were acclimated on low light (LL) and high light (HL) (a and c after Johnsen *et al.* 1994a, see also the present paper for species identification) and field sampling (b and d after Johnsen *et al.* 1998). Field data are pooled for LL- and HL-acclimated phytoplankton obtained from the North Sea, Skagerrak, Ryfylke, Trondheimsfjord, Lofoten and the Norwegian Sea. Note that the Chl c_3 -group indicates ichthyotoxin-producing prymnesiophytes and dinoflagellates (Johnsen *et al.* 1997b)

of physical, chemical and biological variables (Johnsen *et al.* 1997b, Fig. 4). This system has been in use since 1988. The hull contains the power supply and the on-board data processing unit, the communication controller, the algorithms for data analysis and a controller for the Global Data Telemetry and Geo-position Service (ARGOS) or Inmarsat satellite transmission. For the detection of phytoplankton, a Light Beam Attenuation (LBA) meter, equipped with three light-emitting diodes in the blue, green and red part of the visible spectrum, is used (Volent and Johnsen 1993) in combination with an oxygen electrode that can

discriminate between photosynthetic phytoplankton and non-photosynthetic particles. An increase in LBA with a simultaneous rise in oxygen concentration indicates an increase in phytoplankton biomass, in contrast to non-photosynthetic particles, e.g. clay particles, which scatter light and do not produce oxygen (Johnsen *et al.* 1997b).

The Seawatch system has provided a time-series of LBA, oxygen saturation, temperature and salinity, and wind and current speed and direction. The Observer Network, consisting of the local "Fish Farm Observation Network" and Food Hygiene Control Authorities

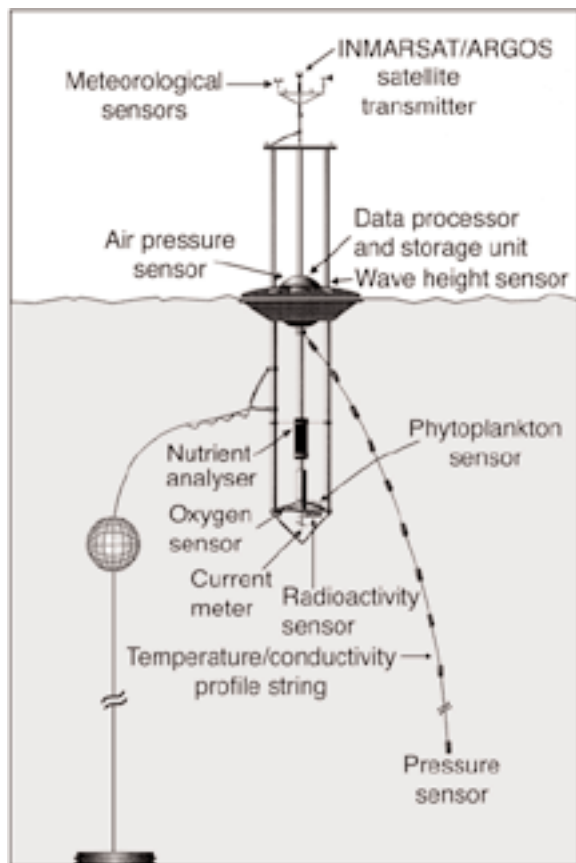


Fig. 4: Seawatch buoy with sensors (after Johnsen *et al.* 1997b)

(Fig. 5), provides additional information. The network provides data on Secchi-disc depth (turbidity and water colour), sea surface temperature, salinity, general weather conditions, fish behaviour and feeding, and unusual biological events such as HABs and high numbers of jellyfish/hydr medusae. Water samples are sent by observers to the relevant authorities for phytoplankton identification and enumeration. The results are presented weekly on the Norwegian algal warning home page on the Internet (Fig. 1). The Norwegian Food Hygiene Control Authorities conduct mussel toxicity tests along the entire Norwegian coast and issue public warnings of HABs (Figs 1, 5).

Detection of a bloom dominated by the dinoflagellate *Ceratium furca* illustrates the potential functioning of the Seawatch system (Fig. 6). A seed stock of *C. furca* was observed in the outer Oslofjord in August/September 1993 (Week 35). During the following

two weeks, this stock was transported northwards along the Norwegian coast, in association with low-salinity water from the Skagerrak, as a consequence of a low-pressure system in the Baltic. High cell numbers of *C. furca* were observed as far north as Trondheim during Week 38. *Dinophysis* spp. were associated with this bloom and were responsible for DSP along the west coast of Norway, and the ichthyotoxic dinoflagellate *Gyrodinium mikimotoi*, which formed a sub-surface bloom in the south (Johnsen *et al.* 1997b).

CASE STUDY OF BIO-OPTICAL PROPERTIES OF PHYTOPLANKTON AND THE DEGRADATION STATUS OF CHLOROPHYLL *a*

To illustrate the use of bio-optics, data were obtained during a spring bloom of the euglenophyte *Eutreptiella gymnastica* in a 19×9×3 m saltwater pool (Fig. 7). Spectral absorption characteristics and corresponding differences in the status of photo-acclimation, and growth as a function of time (six months) were determined. Spectral *in vivo/in vitro* absorption and *in vitro* fluorescence excitation spectra signatures were obtained from glass-fibre filters and compared to isolated chlorophylls and their breakdown products using high-precision liquid chromatography (HPLC) equipped with a fluorescence monitor (spectrofluorometer with flow cell – Johnsen and Sakshaug 1993).

In vivo absorption spectra

Analysis of phytoplankton retained on glass-fibre filters yields valuable information on their spectral absorption and light-scattering properties. The absorption spectra were corrected for scattering of light by particulates, which can be seen at 750–800 nm where absorption by phytoplankton is close to zero. The absorption spectra, obtained using the filter-pad method, are normalized to Chl *a*, as biomass indicator, and corrected for the amplification of the pathlength (see Kirk 1983, Morel and Bricaud 1986, Mitchell 1990, Roesler 1998, for methods and theory). The corrected *in vivo* absorption spectrum normalized to Chl *a* is called the Chl *a*-specific absorption coefficient, $a_{\phi}^*(\lambda)$ (400–700 nm, m²·mg Chl *a*⁻¹, cf. Sakshaug *et al.* 1997 for nomenclature). This coefficient represents the total light absorbed by all pigments, in both photosystems and the corresponding light harvesting complexes (LHC – Johnsen *et al.* 1994b).

Samples from the saltwater pool were analysed immediately. As a result of differences in pigmentation, different pigment groups of phytoplankton could be

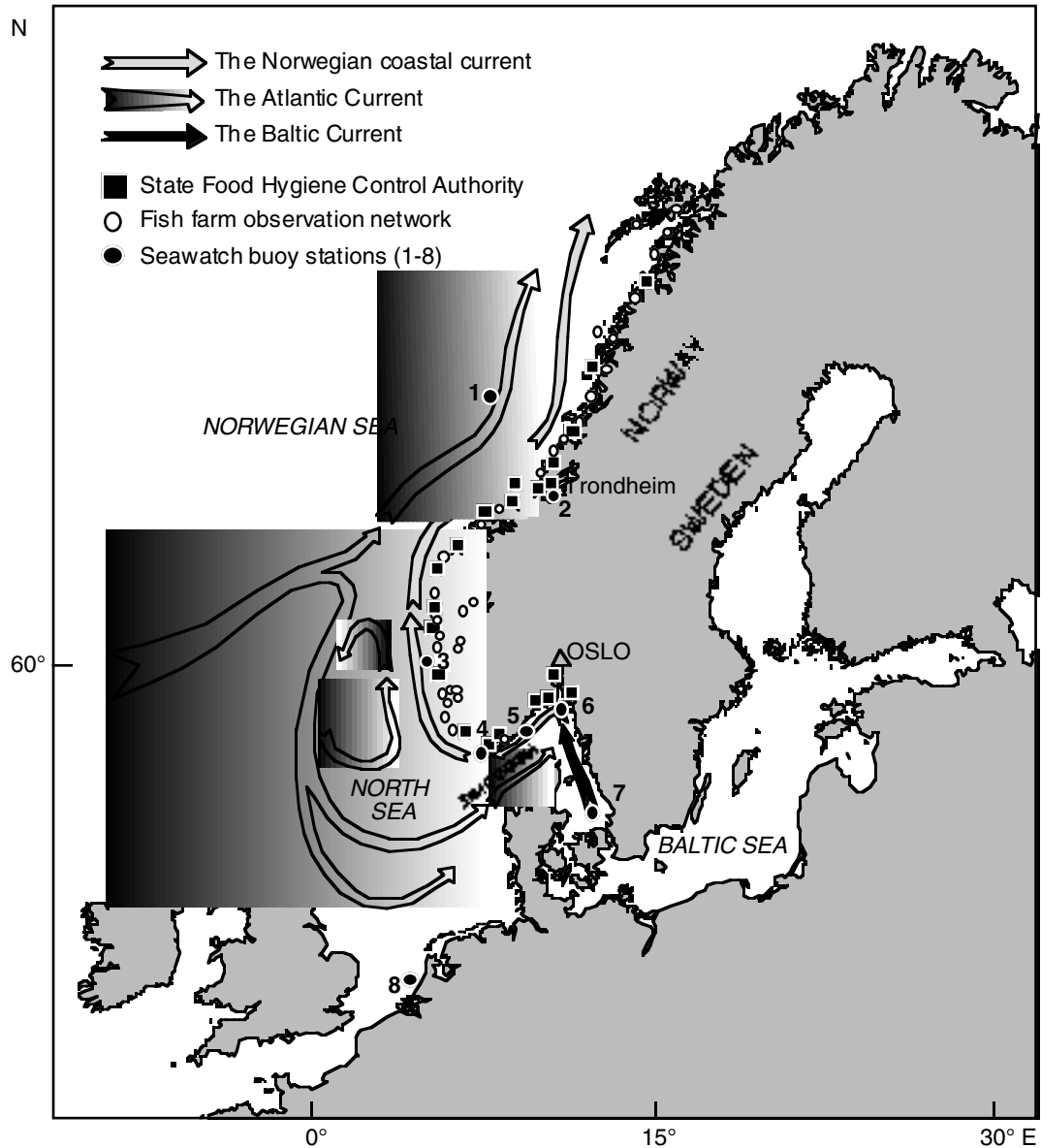


Fig. 5: The Norwegian coastline showing the location of Seawatch buoy stations, the State Food Hygiene Control Authority sites, and fish farm observation network sites. Surface current circulation patterns are indicated (after Johnsen *et al.* 1997b)

separated (Tables I, II, Figs 2, 3, 7). A high level of light scattering in the blue parts of the visible spectrum with a corresponding low absorption by Chl *a* in the red part can clearly be seen during winter, with low phytoplankton biomass (Fig. 7a: 2A–3A, Table II).

The Chl *a*-specific absorption coefficients reflect the fraction of Chl *a* bonded to different pigment proteins in the cell (Johnsen *et al.* 1994b, 1997a). About 60–90% of the cellular Chl *a* in chromophytes (Chl *c*-containing species) may be associated with

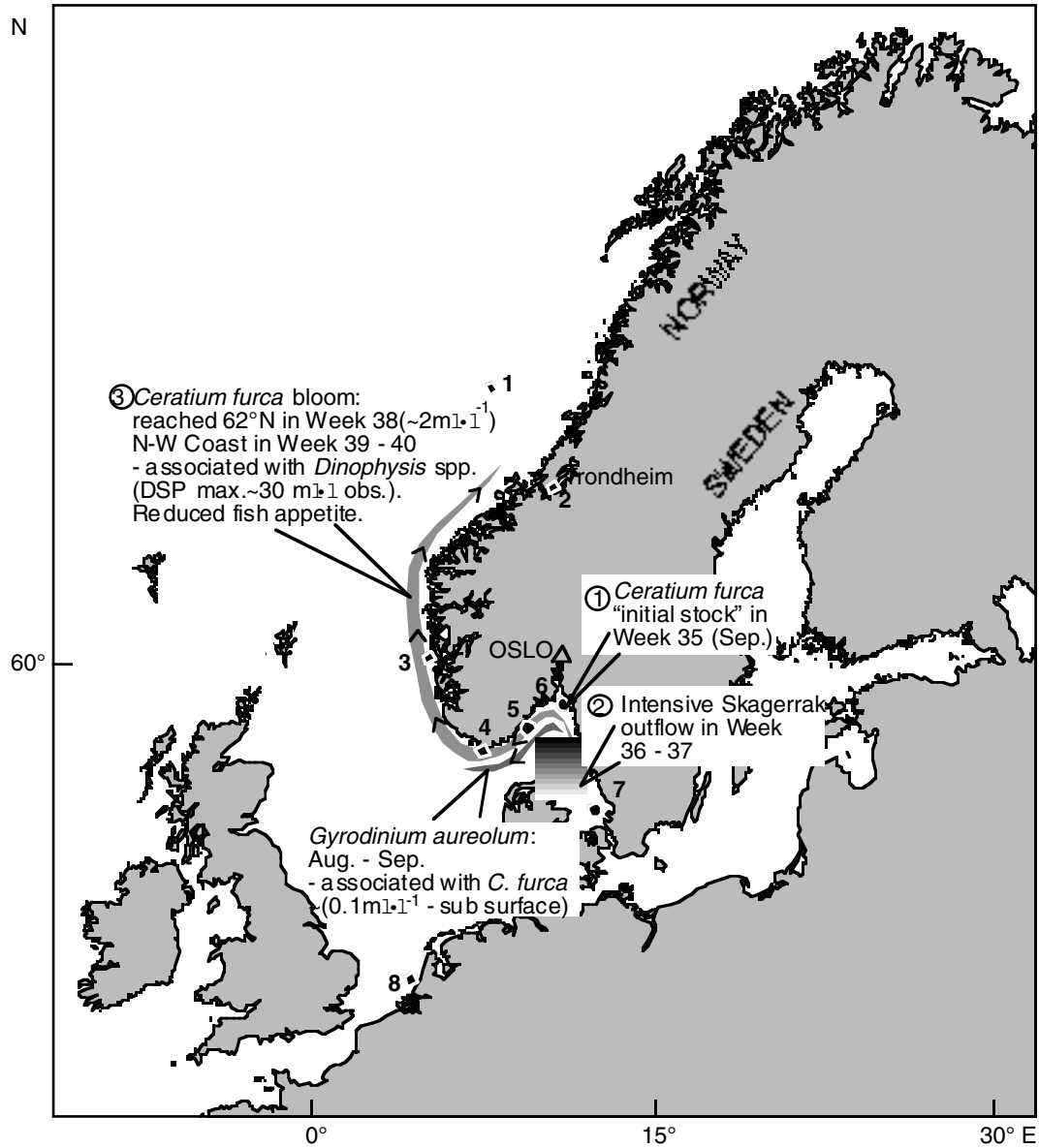


Fig 6: Dinoflagellate blooms along the Norwegian coast during the autumn of 1993 (after Johnsen *et al.* 1997b)

Photosystem (PS) II and its corresponding LHCs, depending on the status of photoacclimation (Johnsen *et al.* 1997a). Johnsen *et al.* (1997a) reported that PS II and the LHCs associated with it have their absorption maxima at 676 and 673–674 nm, with corresponding absorption coefficients at 0.02 (PS II) and from 0.018 to 0.028 (LHC II) m²·mg Chl *a*⁻¹ respectively. In

contrast, the Chl *a*-specific absorption coefficients of isolated and non-denatured PS I are between 0.016–0.019 m²·mg Chl *a*⁻¹, with the red absorption peak (Chl *a* only) situated at 679 nm. These species-specific characteristics are altered through photoacclimation.

In the saltwater pool, species-specific difference in

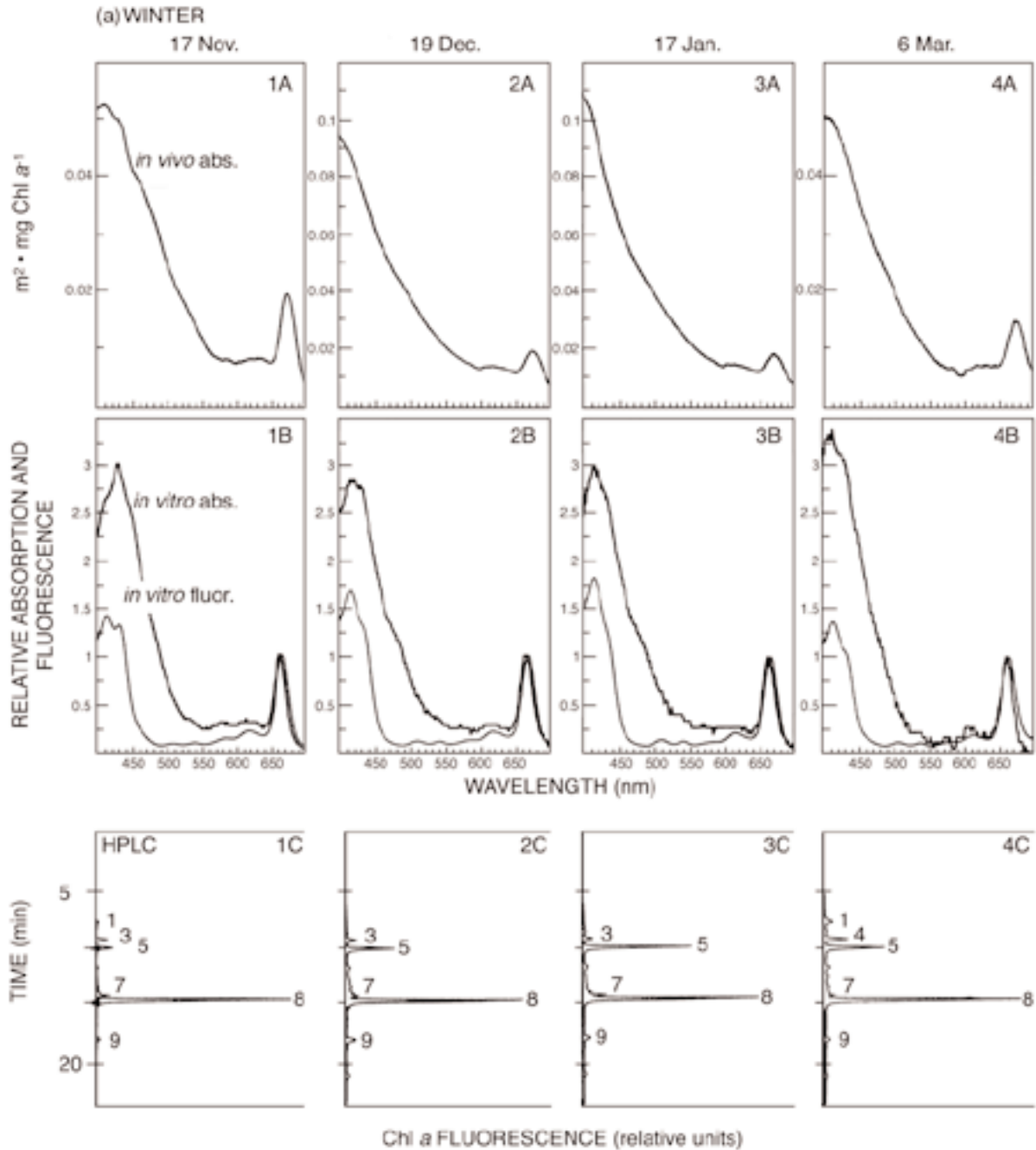


Fig. 7: Bio-optical properties of phytoplankton and the degradation status of Chl *a* versus time in a saltwater pool in Trondheim, Norway (63°N), from (a) 17 November 1989 to 6 March 1990 (winter) and (b) 20 March to 3 May (spring). See Table II for additional information of phytoplankton, detrital matter and pigment status overview. A = Chl *a*-specific *in vivo* absorption coefficients, $a_v(\lambda)$, (see text for explanation). Note scale differences between 1A–4A. B = *in vitro* absorption spectra and fluorescence excitation spectra from the same samples as A. C = HPLC chromatograms of chlorophylls and their degradation status from the same samples as A and B. Peaks 1 = Chl c_{1+2} , 2 = Chlorophyllide *a*, 3 = Phaeophorbide a_1 , 4 = Phaeophorbide a_2 , 5 = Phaeophorbide a_3 , 6 = Chl *b*, 7 = Chl *a*-like, 8 = Chl *a*, 9 = Phaeophytin *a*

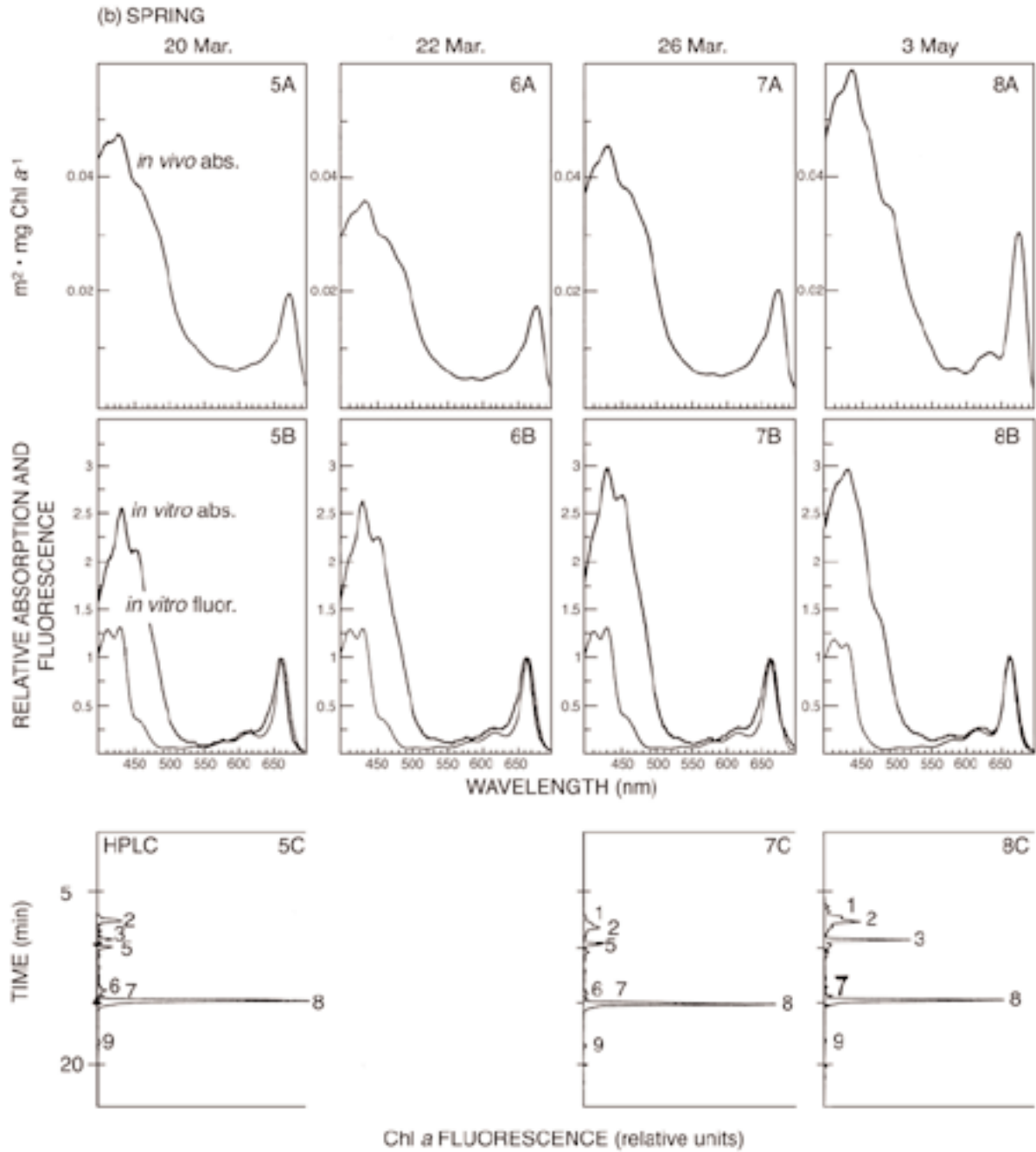


Fig. 7: (continued)

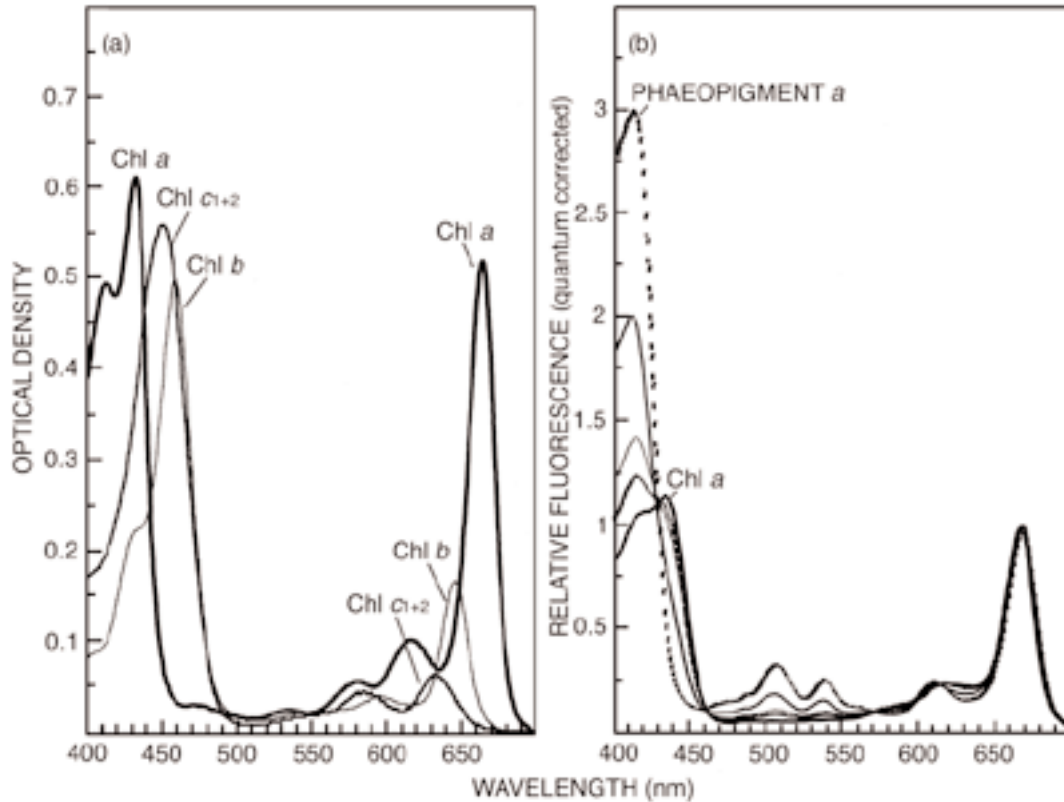


Fig. 8: (a) *In vitro* absorption of chlorophylls in 100% acetone – Chl *a* (peaks at 430, 580, 617, 663 nm), Chl *b* (peaks at 457, 597, 646 nm) and Chl *c*₁₊₂ (peaks at 445, 581, 630 nm); (b) *In vitro* fluorescence excitation spectra from crude pigment extracts in 100% acetone from the diatom *Phaeodactylum tricornutum* treated with different additions of hydrochloric acid (HCl). Samples not treated with HCl gave intact Chl *a*, whereas the extract with the lowest pH gave phaeopigment *a* only (mostly phaeophorbide *a*, with characteristic peaks at 410, 505, 535, 607, 665 nm). See also Johnsen and Sakshaug (1993) and Jeffrey *et al.* (1997)

cells acclimated in high light were characterized by $a_{\phi}^*(675-677 \text{ nm}) > 0.020 \text{ m}^2 \cdot \text{mg Chl } a^{-1}$, whereas cells acclimated to low light generally had values $< 0.020 \text{ m}^2 \cdot \text{mg Chl } a^{-1}$ (Table II). Moreover, Chl *b*-containing phytoplankton, such as *Eutreptiella*, were characterized by an *in vivo* absorption shoulder at 650–655 nm (as a result of absorption by Chl *b*). Low specific absorption coefficients of Chl *a* at 677 nm indicate that a significant part of the cellular Chl *a* is associated with PS I (Table II, Fig. 7b: 5A–7A). Thus, the *in vivo* absorption peaks and shoulders clearly indicate differences in pigmentation and the site where the major fraction of cellular Chl *a* is bonded, i.e. in PS I or II (Fig. 7).

During winter (17 November–17 January), the absorption signal indicates the presence of particulates other than phytoplankton, as revealed by strong light

scattering in the red and a weak pigment signature (Fig. 7a: 1A–4A). In spring, the *E. gymnostica* bloom was characterized by absorption peaks and shoulders at 430 nm (all pigments, especially Chl *a*), 455 nm (Chl *b*), 490 nm (diadinoxanthin), 653 nm (Chl *b*) and 677 nm (Chl *a*, Fig. 7b: 5A–8A). This contrasts with the observed diatom- and chrysophyte-dominated biomass, which have absorption maxima at 430 nm (all pigments, especially Chl *a*), 490 nm (diadinoxanthin), 535 nm (fucoxanthin), 630 nm (Chl *c*) and 675 nm (Chl *a*, Table I).

***In vitro* spectral absorption and fluorescence excitation spectra**

Phytoplankton cells were concentrated onto Whatman

Table II: Bio-optical characteristics in a saltwater pool in Trondheim (63°N) during a 6-month survey from November 1989 to May 1990

Date	<i>In vivo</i> abs. coeff. (m ² -mg Chl a ⁻¹)	λ red peak (nm)	Irradiance at 3 m at noon (μmol·m ⁻² ·s ⁻¹)	Sun angle (degrees)	Chl <i>a</i> (mg·m ⁻³)	Species dominating	Comments
17 Nov.	0.020	673	26	8	1.10	Diatoms + detritus	Medium phaeopigments (phaeo)
19 Dec.	0.019	672	10	3	0.25	Diatoms, dinoflagellates, detritus, tintinnids	Appreciable amount of phaeo
17 Jan.	0.017	673	10	6	0.27	Detritus dominating	The largest phaeo detected
6 Mar.	0.014	673	105	20	0.383	Traces of <i>Eutreptiella</i> sp.	Phaeo lower than in December
20 Mar.	0.019	676	140	27	7.26	<i>E. gymnasctica</i> bloom	Low phaeo + chl <i>b</i>
22 Mar.	0.017	677	120	27	7.64	<i>E. gymnasctica</i> bloom	Low phaeo + chl <i>b</i>
26 Mar.	0.020	677	210	29	8.25	^b <i>E. gymnasctica</i> bloom	Low phaeo + chl <i>b</i>
3 May	0.030	675	—	32	6.71	^c Diatoms + chrysophytes	Medium phaeo and chlorophyllide <i>a</i>

^a An appreciable amount of tintinnids were feeding on phytoplankton

^b A small fraction of *Cochlodinium* sp. was observed

^c The diatom biomass was dominated by *Skeltonema costatum*, *Chaetoceros* spp. An appreciable quantity of chrysophytes, probably belonging to the genus *Apedinella*, were observed with the diatoms

GF/C glass-fibre filters and extracted in cold (0–4°C), 100% acetone for 3 h to prevent chlorophyllase activity. Following this, the concentrate was left for a further 21 h in 90% acetone to ensure efficient extraction of the polar pigments. The Chl *a* concentration for all preparations was estimated according to Jeffrey and Humphrey (1975). Instead of measuring Chl *a* only at the red absorption maximum, and correcting for blank measurement, an *in vitro* absorption spectrum can be obtained from 400–700 nm for each sample. The extract can then be diluted using the same solvent and measured in a spectrofluorometer to obtain an *in vitro* fluorescence excitation spectra (relative units). Whereas *in vitro* absorption spectra reflect the total pigment composition, the corresponding *in vitro* fluorescence excitation spectra (excitation 400–700 nm, emission 730 nm) reflect Chl *a* only and its degradation products (Johnsen and Sakshaug 1993). This information can be used as a quick, simple and inexpensive alternative to HPLC. The degradation status of chlorophylls was measured using the HPLC system described by Johnsen and Sakshaug (1993). The different chlorophyll fractions were detected in a spectrofluorometer fitted with a flow cell. The spectral characteristics of each component were quantum-corrected before identification. The data from the HPLC connected to the fluorescence detector are shown in Figure 7 (1–8C) and are in agreement with the data obtained from *in vitro* absorption and fluorescence.

Using the fluorescence excitation spectrum system described above, there is almost no fluorescence signal from the Chl *c* group, and Chl *b* can only be seen as a shoulder at around 460 nm (Fig. 7b: 5B–7B, Fig. 8). The *in vitro* red peaks for absorption and fluorescence have different shapes when comparing chromophytes and Chl *b*-containing algae, as seen from the *in vitro* spectra of *Eutreptiella* sp. Compared to those of diatoms and chrysophytes (Fig. 7b: 5B–8B). This difference reflects the broadening of the red peak absorption from 640 to 650 nm by Chl *b*, which cannot be seen in the corresponding fluorescence excitation spectrum, because the emission from Chl *b* is extremely low at 730 nm when excited with light from 640 to 650 nm.

The optical density, OD (λ), indicates the different absorption properties of Chl *a*, and Chl *c*₁₊₂ (source: the diatom *Phaeodactylum tricoratum*) and Chl *b* (source: the prasinophyte *Micromonas pusilla*) in acetone (Fig. 8a). The pigments were isolated by thin-layer chromatography (cellulose plates) using the method of Jeffrey (1968). The corresponding fluorescence excitation spectrum indicates the different optical characteristics between intact Chl *a* (blue peak at 431 nm) and phaeophorbide *a*; a result of the Chl *a* molecule losing the magnesium atom and phytol chain (characteristic peaks situated at 410, 505 and 535 nm – Fig. 8b, cf. Jeffrey *et al.* 1997). These optical

characteristics clearly reflect the findings from the HPLC analyses using fluorescence excitation at 420 nm and emission at 685 nm (Fig. 7a, b: 1C–8C).

In Trondheim at 63°N, the maximum irradiance is highly affected by sun angle, cloud cover and time of year (Table II). The pigment-group specific differences in Chl *a*-specific absorption coefficients are related to the light history: variability in daylength, and the intensity and spectral distribution of the irradiance. Because most Chl *b*-containing phytoplankton classes (chlorophytes, prasinophytes and euglenophytes) contain a considerable quantity of Chl *a* bonded to PS I, this implies long-wave absorption of Chl *a* in the red part of the spectrum, i.e. 677–678 nm and corresponding absorption coefficients $<0.02 \text{ m}^2\text{-mg Chl } a^{-1}$ for cells acclimated to high light (cf. Johnsen *et al.* 1997a). The *in vivo* absorption spectra of Chl *b*-containing *Eutreptiella gymnastica* indicated that a larger fraction of their Chl *a* is associated with PS I. The *in vivo* red absorption maxima of 677 nm for Chl *b*-containing *Eutreptiella* sp. in March, differs from the absorption maxima of 672–675 nm for chromophyte-dominated water samples, indicating that most of the cellular Chl *a* was associated with PS II and their corresponding LHCs for the latter (Table II, Johnsen *et al.* 1997a). Winter low concentrations of $0.38 \text{ mg}\cdot\text{Chl } a \text{ m}^{-3}$ were found at the onset of the bloom on 6 March. Two weeks later, peaks of up to $8 \text{ mg Chl } a \text{ m}^{-3}$ were attained (Table II). This bloom is closely linked to changes in the irradiance field and takes place when the seawater temperature is at its minimum (approx. 4–6°C).

CONCLUSION

The combined use of *in vivo* and *in vitro* absorption and fluorescence excitation spectra provides information on the presence of different groups of phytoplankton, distinguished by their pigments (bio-optical taxonomy). Basic information is also provided for primary production models (fraction of light available for photosynthesis) and an indication of the status of growth of the cell is given. The status of health of the phytoplankton population can be traced by examining the degradation of Chl *a* using the methods described herein. This information can be obtained from analysing phytoplankton and other particles collected on glass-fibre filters, wrapped in aluminum foil and stored at -20°C for spectrophotometric and spectrofluorometric detection of the pigments and their corresponding state of degradation.

LITERATURE CITED

- BRICAUD, A., BEDHOMME, A.-L. and A. MOREL 1988 — Optical properties of diverse phytoplanktonic species: experimental results and theoretical interpretation. *J. Plankt. Res.* **10**: 851–873.
- CULLEN, J. J. and M. R. LEWIS 1995 — Biological processes and optical measurements near the sea surface: some issues relevant to remote sensing. *J. geophys. Res.* **100**(C7): 13255–13266.
- HAXO, F. T. and L. R. BLINKS 1950 — Photosynthetic action spectra of marine algae. *J. gen. Physiol.* **33**: 389–422.
- JEFFREY, S. W. 1968 — Quantitative thin-layer chromatography of chlorophylls and carotenoids from marine algae. *Biochim. Biophys. Acta* **162**: 271–285.
- JEFFREY, S. W. and G. F. HUMPHREY 1975 — New spectrophotometric equations for determining chlorophylls *a*, *b*, *c*₁ and *c*₂ in algae, phytoplankton and higher plants. *Biochem. Physiol. Pfl.* **167**: 191–194.
- JEFFREY, S. W., MANTOURA, R. F. C. and T. BJØRNLAND 1997 — Data for the identification of 47 key phytoplankton pigments. In *Phytoplankton Pigments in Oceanography: Guidelines to Modern Methods*. Jeffrey, S. W., Mantoura, R. F. C. and S. W. Wright (Eds). Paris: UNESCO: 449–559.
- JOHNSEN, G., NELSON, N. B., JOVINE, R. V. M. and B. B. PRÉZELIN 1994b — Chromoprotein- and pigment-dependent modeling of spectral light absorption in two dinoflagellates, *Prorocentrum minimum* and *Heterocapsa pygmaea*. *Mar. Ecol. Prog. Ser.* **114**: 245–258.
- JOHNSEN, G., PRÉZELIN, B. B. and R. V. M. JOVINE 1997a — Fluorescence excitation spectra and light utilization in two red tide dinoflagellates. *Limnol. Oceanogr.* **42**: 1166–1177.
- JOHNSEN, G. and E. SAKSHAUG 1993 — Bio-optical characteristics and photoadaptive responses in the toxic and bloom-forming dinoflagellates *Gyrodinium aureolum*, *Gymnodinium galatheanum*, and two strains of *Prorocentrum minimum*. *J. Phycol.* **29**: 627–642.
- JOHNSEN, G., SAMSET, O., GRANSKOG, L. and E. SAKSHAUG 1994a — *In vivo* absorption characteristics in 10 classes of bloom-forming phytoplankton: taxonomic characteristics and responses to photoadaptation by means of discriminant and HPLC analysis. *Mar. Ecol. Prog. Ser.* **105**: 149–157.
- JOHNSEN, G., SAMSET, O. and E. SAKSHAUG 1998 — Bio-optical classification of potential harmful chlorophyll *c*₃-containing prymnesiophyte blooms in Scandinavian waters. In *Harmful Microalgae*. Reguera, B., Blanco, J., Fernández, M. L. and T. Wyatt (Eds). Paris: Intergovernmental Oceanographic Commission of UNESCO: 300–304.
- JOHNSEN, G., VOLENT, Z., TANGEN, K. and E. SAKSHAUG 1997b — Time series of harmful and benign phytoplankton blooms in northwest European waters using the Seawatch buoy system. In *Monitoring Algal Blooms: New Techniques for Detecting Large-Scale Environmental Change*. Kahru, M. and C. Brown (Eds). Austin, Texas: Springer-Verlag and Landes Bioscience: 115–143.
- KIRK, J. T. O. (Ed.) 1983 — *Light and Photosynthesis in Aquatic Ecosystems*. Cambridge; University Press: 401 pp.
- MITCHELL, B. G. 1990 — Algorithms for determining the absorption coefficient of aquatic particulates using the Quantitative Filter Technique (QFT). SPIE. *Ocean Optics* **1302**: 137–48.
- MOREL, A. and A. BRICAUD 1986 — Inherent optical properties of algal cells including picoplankton: theoretical and experi-

- mental results. In *Photosynthetic Picoplankton*. Platt, T. and W. K. W. Li (Eds). *Can. Bull. Fish. aquat. Sci.* **214**: 521–559.
- ROESLER, C. S. 1998 — Theoretical and experimental approaches to improve the accuracy of particulate absorption coefficients derived from the quantitative filter technique. *Limnol. Oceanogr.* **43**: 1649–1660.
- SAKSHAUG, E., BRICAUD, A., DANDONNEAU, Y., FALKOWSKI, P. G., KIEFER, D. A., LEGENDRE, L., MOREL, A., PARSLow, J. and M. TAKAHASHI 1997 — Parameters of photosynthesis: definitions, theory and interpretation of results. *J. Plankt. Res.* **19**: 1637–1670.
- UNESCO 1996 — Design and implementation of harmful algal monitoring systems. Anderson, P. (Ed.). Intergovernmental Oceanographic Commission Technical Series. No. **44**: 102 pp.
- VOLANT, Z. and G. JOHNSEN 1993 — Presentation of an optical sensor – “Optisens” designed for eulerian measurements of phytoplankton on a moored buoy. In *International Symposium in High Latitude Optics*. Eilertsen, H. C. (Ed.). Bellingham, Washington; International Society for Optical Engineering **2048**: 138-147.
- YENTSCH, C. S. and C. M. YENTSCH 1979 — Fluorescence spectral signatures: The characterization of phytoplankton populations by use of excitation and emission spectra. *J.*